9-16-2013

Isolation of high quality graphene from Ru by solution phase intercalation

E. Koren
Brookhaven National Laboratory

Eli A. Sutter
University of Nebraska–Lincoln, esutter@unl.edu

S. Bliznakov
Brookhaven National Laboratory

F. Ivars-Barcelo
Brookhaven National Laboratory

P. Sutter
Brookhaven National Laboratory, psutter@unl.edu

Follow this and additional works at: http://digitalcommons.unl.edu/electricalengineeringfacpub

Part of the Computer Engineering Commons, and the Electrical and Computer Engineering Commons

Isolation of high quality graphene from Ru by solution phase intercalation

E. Koren, E. Sutter, S. Bliznakov, F. Ivars-Barcelo, and P. Sutter

---

Articles you may be interested in

Frame assisted H$_2$O electrolysis induced H$_2$ bubbling transfer of large area graphene grown by chemical vapor deposition on Cu
Applied Physics Letters **102**, 022101 (2013); 10.1063/1.4775583

Microscopic mechanisms of graphene electrolytic delamination from metal substrates
Applied Physics Letters **104**, 233105 (2014); 10.1063/1.4882165

WSXM: A software for scanning probe microscopy and a tool for nanotechnology
Review of Scientific Instruments **78**, 013705 (2007); 10.1063/1.2432410

Scanning tunneling microscopy on epitaxial bilayer graphene on ruthenium (0001)
Applied Physics Letters **94**, 133101 (2009); 10.1063/1.3106057

Intercalation of metal islands and films at the interface of epitaxially grown graphene and Ru(0001) surfaces
Applied Physics Letters **99**, 163107 (2011); 10.1063/1.3653241

Silicon intercalation at the interface of graphene and Ir(111)
Applied Physics Letters **100**, 083101 (2012); 10.1063/1.3687688

Isolation of high quality graphene from Ru by solution phase intercalation

E. Koren,[1] E. Sutter,[1] S. Bliznakov,[2] F. Ivars-Barcelo,[1] and P. Sutter[1,a)]

[1]*Center for Functional Nanomaterials, Brookhaven National Laboratory, Upton, New York 11973, USA*
[2]*Chemistry Department, Brookhaven National Laboratory, Upton, New York 11973, USA*

We introduce a method for isolating graphene grown on epitaxial Ru(0001)/α-Al$_2$O$_3$. The strong graphene/Ru(0001) coupling is weakened by electrochemically driven intercalation of hydrogen underpotentially deposited in aqueous KOH solution, which allows the penetration of water molecules at the graphene/Ru(0001) interface. Following these electrochemically driven processes, the graphene can be isolated by electrochemical hydrogen evolution and transferred to arbitrary supports. Raman and transport measurements demonstrate the high quality of the transferred graphene. Our results show that intercalation, typically carried out in vacuum, can be extended to solution environments for graphene processing under ambient conditions. © 2013 AIP Publishing LLC. [http://dx.doi.org/10.1063/1.4821269]

Graphene, a two-dimensional honeycomb lattice of sp^2-bonded carbon atoms, has attracted high interest since its first isolation from graphite.[1] Attributes such as very high intrinsic carrier mobilities,[2] optical transparency,[3] extreme tensile strength,[4] and stability[5,6] make graphene a promising candidate for applications in electronics, spintronics, optoelectronics, sensing, energy storage, etc. Monolayer and few-layer graphene with high crystal quality were realized by graphite exfoliation,[1,7] thermal decomposition of SiC,[8] and more recently carbon segregation and chemical vapor deposition (CVD) growth on catalytic metals, such as Ru,[9] Pt,[10,11] Ni,[12,13] and Cu.[14–16] Most applications require high-quality wafer size graphene films transferable to arbitrary substrates. The conventional method for producing transferable CVD graphene is growth on foils or thin films of non-noble transition metals, followed by the deposition of a stabilizing polymer layer and etching of the metal substrate to isolate the graphene. An interesting alternative is transfer by electrochemical hydrogen evolution beneath the graphene film, which has been recently demonstrated for Cu[16] and Pt.[11] Graphene grown on Cu foils and Pt(111) single crystals could be transferred non-destructively in this way, allowing the repeated reuse of the metal substrates. A key aspect of this method appears to be the very weak graphene-metal coupling[10] common to both Cu and Pt, which allows the solution (or H) to penetrate at the graphene-metal interface and facilitates the transfer by hydrogen evolution.

Here, we discuss the transfer of graphene from epitaxial Ru(0001). Growth by carbon segregation on Ru(0001) gives rise to very high quality monolayer graphene with macroscopic domain sizes, a rotational alignment of the graphene domains that avoids high-angle boundaries,[9] as well as few-layer graphene with layer-by-layer thickness control.[17] Recently, we have shown that this growth method can be scaled up by using polycrystalline Ru thin films on SiO$_2$/Si[18] or epitaxial Ru(0001) films on c-axis sapphire (α-Al$_2$O$_3$ (0001)).[19] Epitaxial Ru/Al$_2$O$_3$, in particular, offers an ordered, atomically flat and monocrystalline (i.e., grain boundary free)

metal template for graphene growth. Besides showing the characteristics, such as large graphene domain size and low defect density, observed on Ru single crystals, the interstitial carbon solubility on these epitaxial templates is tunable via the Ru film thickness, which allows the growth of pure mono-layer graphene by hydrocarbon CVD.[20] The transfer of graphene from Ru has remained a challenge to date. Ru is more difficult to etch than less noble transition metals, and although initial attempts at wet-chemical etching of Ru have allowed graphene isolation, they have so far resulted in elevated defect densities.[19] Given the higher cost of Ru, a non-destructive transfer method that does not involve metal etching, similar to that demonstrated for Pt(111),[11] would be desirable. However, the strong interfacial interaction between graphene and Ru(0001)[21] implies a tight coupling and small separation between the as-grown graphene and the metal substrate, as shown theoretically[22] and experimentally,[23] and it is unlikely that such an interface would allow a separation by hydrogen evolution. Oxygen intercalation has been shown to weaken the interfacial coupling,[24,25] and water vapor similarly intercalates at the graphene/Ru interface,[26] but these processes have so far only been demonstrated under ultrahigh vacuum (UHV) conditions, which are not suitable for large-scale processing.

To identify a non-destructive method for transferring graphene from Ru(0001)/Al$_2$O$_3$ that is scalable and can be carried out under ambient conditions—and hence can be performed routinely in any laboratory—we have focused on electrochemical approaches in aqueous solutions. The isolation method described here is based on a two-step process. In a first step, a low negative voltage is applied to the graphene-covered Ru electrode in two-electrode configuration in 0.2 M KOH solution. At cathodic potentials in the range 0.05–0.4 V more positive than the onset potential for H$_2$ evolution, overlapping of H underpotential deposition (UPD) and surface oxide/hydroxide reduction reactions are observed on Ru and the other platinum group metals in both acid and alkaline electrolytes.[27–29] As a result of these electrochemical processes, a rapid large-scale intercalation of UPD hydrogen is first forming at the edges where Ru is in contact with the electrolyte and then diffuses at the metal-graphene interface, which weakens the interfacial coupling and allows a thin

a)Author to whom correspondence should be addressed. Electronic mail: psutter@bnl.gov.

film of water molecules to penetrate at the interface and chemisorb onto H adsorbed Ru surface.[30] In the second step, a larger negative voltage is applied and the graphene is separated from the substrate by electrochemical hydrogen evolution and can then be transferred to an arbitrary support. The properties of graphene transferred from Ru to SiO_2/Si are characterized by Raman spectroscopy and Raman mapping, and by transport measurements on back-gated field-effect devices. Our results show that high quality graphene with low defect density and high carrier mobility can be isolated from Ru(0001). The Ru/Al_2O_3 template remains intact and should be re-usable repeatedly for further graphene growth.

Graphene was grown by high-temperature exposure to ethylene on 850 nm Ru(0001)/Al_2O_3 substrates, as described previously.[19,20] Completed monolayers as well as partial graphene layers consisting of uncoalesced large monolayer domains were used for this study. The Ru substrates before and after graphene growth and transfer were characterized by tapping-mode atomic force microscopy (AFM) and Raman spectroscopy. Following graphene growth, the samples were spin-coated with a poly-(methyl methacrylate) (PMMA) stabilization layer. Graphene isolation experiments were performed on such samples in aqueous 0.2 M KOH (99.99% purity, Sigma-Aldrich) solution. The solution process used an electrochemical cell with a Pt foil counter electrode and a Bio-Logic SP-150 potentiostat. The progress of graphene isolation was recorded in real time using optical video microscopy. The isolated graphene was transferred onto 300 nm SiO_2 on degenerately doped Si for Raman characterization and electrical device fabrication. Raman spectra and spatially resolved maps were obtained using a commercial confocal Raman microscope (WiTec Alpha) at an excitation wavelength of 532 nm and incident power below 1 mW. A 100× objective provided a diffraction-limited spot size of about 500 nm. Device fabrication was carried out using standard electron-beam lithography. To establish contacts, 5 nm Cr followed by 45 nm Au were evaporated onto the graphene. Two lithography steps were conducted for contact fabrication and for defining the graphene channel, respectively, using PMMA as the resist. The PMMA was dissolved in acetone, and the patterned samples were vacuum-annealed at 200 °C for several hours. Consequently, tens of similar graphene based field effect transistors with channel size of $10 \times 10 \, \mu m^2$ were established and characterized by back-gated field-effect transport.

Figure 1 shows real-time observations during the first step of our graphene transfer process from Ru/Al_2O_3, the low-bias electrochemical intercalation of UPD H followed by the penetration of H_2O molecules at the graphene/Ru(0001) interface in aqueous solution. The graphene/PMMA-covered epitaxial Ru film acting as the working electrode is immersed in 0.2 M KOH solution and biased to −1 V relative to the grounded Pt counter electrode; this applied bias is below the measured threshold for H_2 evolution (∼−1.3 V). The evolution of the sample under these conditions is illustrated in a time-lapse series of optical images (Figs. 1(a)–1(d)) of a small part of a sample that is covered by large monolayer graphene domains, as verified by low-energy electron microscopy.[20] To facilitate access of the solution, the Ru at the sample edges has been exposed by
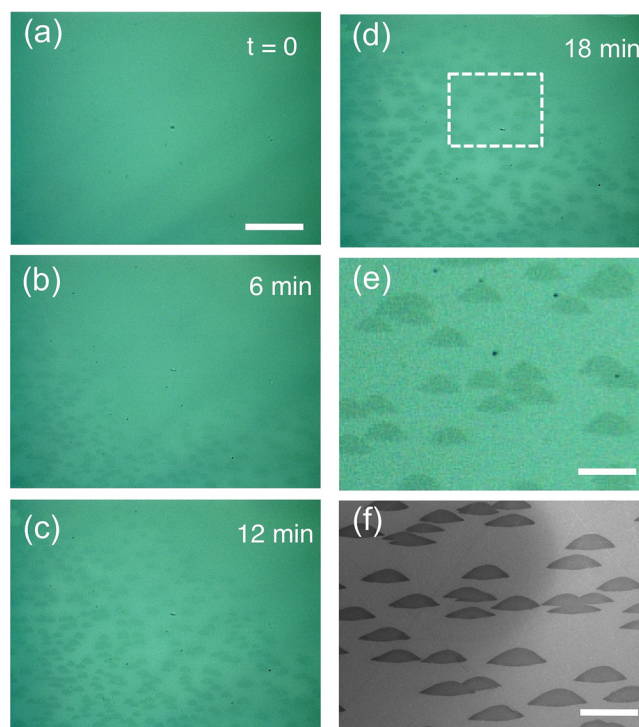

FIG. 1. Electrochemical intercalation of graphene/Ru(0001). (a)–(d) Time-lapse series of optical images of the PMMA/Graphene/Ru electrode before (a) and during ((b)–(d)) the electrochemical induced hydrogen UPD intercalation at the Graphene/Ru interface in 0.2 M KOH solution, with a voltage of −1 V applied to the Ru relative to the grounded Pt foil counter electrode. Elapsed time as given in the images; scale bar: 500 μm. (e) Higher magnification image of the rectangular section marked in (e). Scale bar: 100 μm. (f) UHV scanning electron microscopy image of a sample with similar partial graphene coverage. Scale bar: 100 μm.

locally removing the PMMA. Before applying the bias voltage to initiate the electrochemical processes (Fig. 1(a)), optical microscopy shows very little contrast and a uniform appearance of the sample; in particular, the graphene domains on the Ru substrate are not visible optically. Few minutes after applying the bias (Fig. 1(b)), contrast begins to develop and an array of graphene domains becomes visible at the lower left corner of the image. At this stage, most of the sample surface still shows uniform appearance without significant optical contrast. The boundary of the contrast region sweeps gradually across the field of view (Fig. 1(c)) until, after about 18 min of processing, graphene domains are visible in the entire image (Fig. 1(d)). A higher magnification view (Fig. 1(e)) clearly shows lens-shaped darker areas with average length of the order of 100 μm. Comparison with a scanning electron microscopy image of a similar sample (Fig. 1(f)) unambiguously identifies these darker regions as graphene domains.

The observed increase in contrast indicates a change in the optical properties of the metal/graphene/PMMA sandwich structure induced by the application of a small negative bias in the aqueous KOH solution. Such changes are not observed even after prolonged immersion in the solution at zero bias. Moreover, in optical microscopy in air or solution, with or without the PMMA capping layer, there is no significant contrast between graphene and the underlying Ru. We thus explain the appearance of contrast in our experiment by the buildup of a film of electrolyte that penetrates between

the graphene flakes and the Ru when the system is biased, thus adding a layer with different refractive index that provides contrast and allows the individual graphene domains to be observed in optical microscopy. Such optical contrast is not observed for samples in which, instead of the electrochemical intercalation, the graphene has been oxygen-intercalated in vacuum, which gives rise to an atomic layer of adsorbed O on the Ru(0001) surface beneath graphene.[24,25] This difference in behavior supports our conclusion that the present experiments in an electrochemical cell involve the penetration of a thicker film of the electrolyte at the graphene/Ru interface, which changes the optical properties sufficiently to produce the contrast seen in Fig. 1.

The associated decoupling of graphene from the metal by this electrochemically driven solution phase penetration is confirmed by the implementation of the second step of our transfer process, which involves electrochemical hydrogen evolution to separate the PMMA stabilized graphene macroscopically from the Ru substrate. The conditions in this process step follow those used previously for the isolation of graphene from Pt(111):[11] Brief application of a high negative (-10 V) bias voltage to the Ru working electrode causes H_2 evolution, visible via bubbles in the solution. H_2 generated on Ru lifts the graphene/PMMA film off the metal such that it can be deposited on SiO_2/Si or any other substrate. The overall two-step transfer process of graphene on Ru(0001), consisting of electrochemically driven intercalation and electrolyte penetration followed by separation via H_2 evolution, is illustrated schematically in Fig. 2. The intercalation and decoupling of the graphene from the Ru substrate in electrolyte solution (Fig. 2(a)) extends previous intercalation experiments in vacuum using exposure to gases,[24,25] vapors,[26] or by evaporation of metals or semiconductors[31]

and thus makes intercalation available as a tool for large-scale processing under ambient conditions.

The described process enables us to mechanically transfer PMMA-stabilized graphene from epitaxial Ru(0001)/ Al_2O_3 growth templates onto any other substrate. For further characterization, we performed transfers to SiO_2/Si for both Raman spectroscopy and transport measurements. Fig. 3(a) shows an intensity map of the 2D Raman band; Fig. 3(b) displays corresponding Raman spectra taken at different points in the transferred graphene flakes. The Raman spectra generally show 2D/G band intensity ratios of $\sim$1.5–2.5. A single Lorentzian lineshape of the 2D band (FWHM ~ 36 cm^{-1}) confirms the presence of monolayer graphene.[32] The defect-related D band generally shows low intensity (Fig. 3(b)), with 2D/D intensity ratios between 15 and 60. We note that the 2D/D ratio is locally reduced at specific points within the graphene domains, which are identified as the graphene nucleation sites by comparison to real-time low-energy electron microscopy movies. The likely cause for this elevated defect density is the presence of residual surface contaminants on the Ru films, which may be gettered during the initial nucleation of the large graphene domains. Future work will be devoted to reducing the impurity concentration and hence eliminate the associated defects. These studies will be facilitated by the ability to perform a broader range of characterization (e.g., micro-Raman) on isolated or transferred graphene samples.

Figures 3(c) and 3(d) show representative transport characteristics of field-effect devices fabricated from graphene transferred from Ru(0001)/Al_2O_3 to 300 nm SiO_2/Si. Optical microscopy shows the typical optical contrast of the exposed $10\,\mu$m $\times$ $10\,\mu$m graphene channel, whose location is confirmed by 2D Raman intensity mapping (Fig. 3(c)). The resistance as a function of back-gate voltage of this field-effect
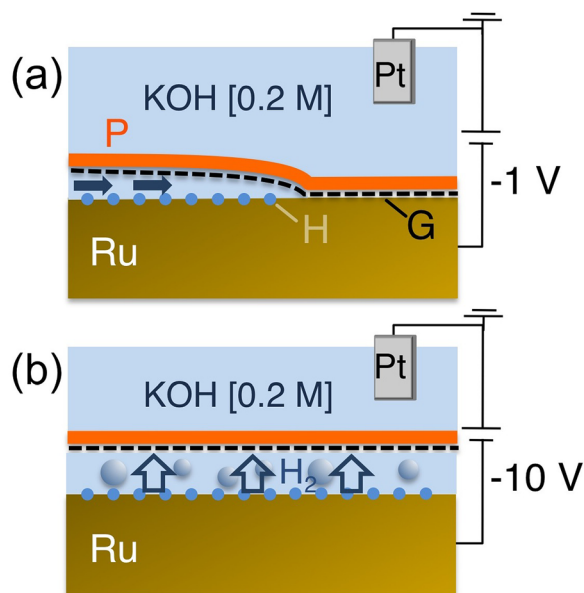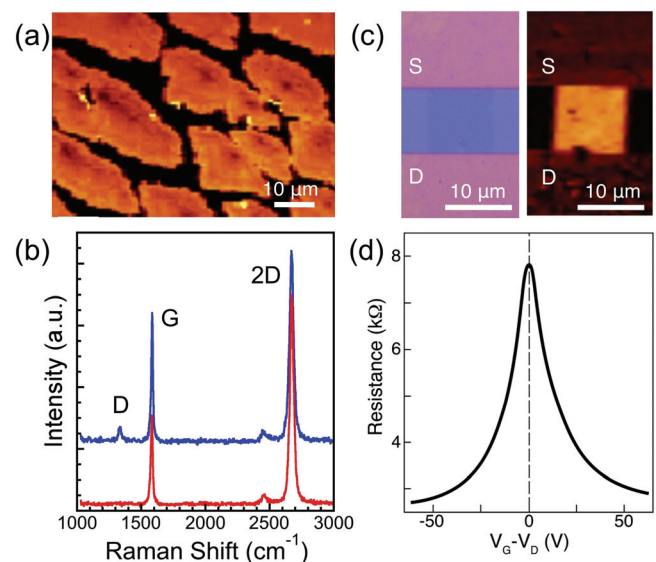

FIG. 2. Two-step electrochemical transfer of graphene from epitaxial Ru(0001)/Al_2O_3. (a) Schematic illustration of the low-voltage (-1 V) underpotential deposition of hydrogen on Ru(0001), followed by the penetration of the electrolyte at the graphene/Ru interface (G: monolayer graphene; P: PMMA polymer stabilization layer). (b) Separation of the graphene/PMMA film from the Ru substrate by brief (<1 min) biasing to -10 V, which causes H_2 evolution.

FIG. 3. Properties of graphene transferred from Ru(0001) to SiO_2/Si. (a) Map of the 2D Raman band intensity at (2670 ± 10) cm^{-1} of transferred arrays of graphene domains. (b) Individual Raman spectra of the same sample. (c) Optical image and 2D Raman intensity map of a back-gated field effect device with $10\,\mu$m $\times$ $10\,\mu$m channel, supported on 300 nm SiO_2/Si. The open graphene channel is visible between the Au/Cr source (S) and drain (D) contacts. (d) Typical room temperature gated transport characteristic (S-D resistance versus back-gate voltage) of such field-effect devices.

transistor is shown in Fig. 3(d). For this and several similar devices, we observe the Dirac point at a back gate voltage of 3 ± 1 V, and we extract a minimum charge carrier mobility of 4×10^3 cm^2 V^{-1} s^{-1} at a carrier density of 2.5×10^{11} cm^{-2}. Our extracted charge carrier mobility compares well with previous reports for transferred CVD graphene on SiO$_2$ for which room temperature field-effect mobility values in the range of 10^3 to over 10^4 cm^2 V^{-1} s^{-1} were reported.[14,33,34] As in these other cases, finite substrate roughness and trapped charge in the oxide are the likely main reasons for the limited mobility,[35] highlighting the importance of supporting graphene devices on other dielectrics, such as h-BN.[36]

A potential advantage of a non-destructive graphene transfer method that avoids metal etching is the repeated re-usability of the substrates, which is especially important if noble metals such as Ru are used for graphene growth. To further explore this possibility, we characterized the Ru/Al$_2$O$_3$ substrates before and after graphene growth and transfer. For the starting Ru thin film substrate, AFM shows a surface with flat terraces separated by atomic steps (Fig. 4(a)). Following graphene growth and transfer by solution-phase intercalation and H evolution, a clean surface with a well-defined terrace and step morphology is readily recovered by annealing in vacuum (Fig. 4(b)). Raman spectroscopy shows only the TO phonon of Ru but no other spectral lines that could be attributed to contaminants (Fig. 4(c)). These findings suggest that ordered, clean Ru(0001) surfaces with atomically flat terraces are readily recovered after graphene growth and transfer from the Ru/Al$_2$O$_3$ thin films.

In summary, we have presented a method for isolating CVD-grown graphene from epitaxial Ru(0001)/Al$_2$O$_3$ substrates. The method avoids the commonly used etching of the metal template and instead uses a two-step electrochemical process to non-destructively separate graphene from the metal substrate. The key step is an electrochemically driven hydrogen UPD intercalation of the graphene/Ru interface in aqueous solution, which weakens the strong interaction of as-grown graphene with the Ru substrate and allows H$_2$O molecules to penetrate and chemisorb onto the H adsorbed Ru surface. Subsequent electrochemical hydrogen evolution induces a macroscopic separation between graphene and metal, effectively isolating the graphene and enabling its transfer to arbitrary supports. Our work extends intercalation processes, which have so far been carried out primarily in vacuum, to solution environments. This sets the stage for the use of electrochemically driven chemical reactions, etching, and deposition/plating for the controlled large-scale processing of different graphene/metal systems under ambient conditions.
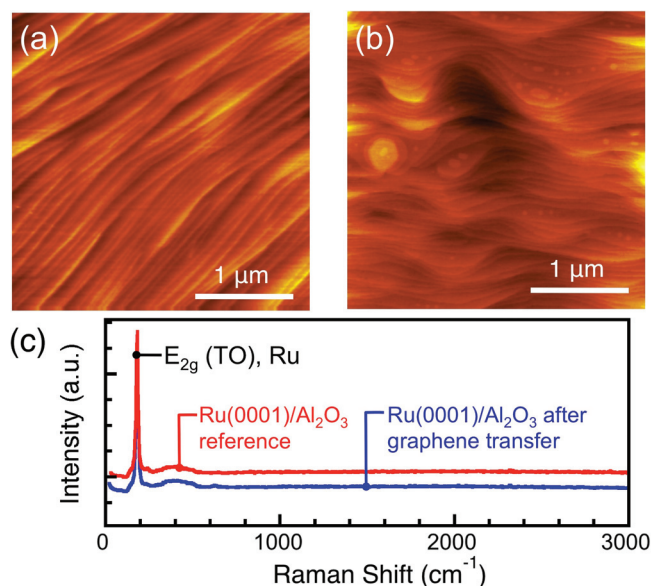
FIG. 4. Surface characterization of Ru(0001)/Al$_2$O$_3$(0001) films before and after graphene transfer. (a) Tapping mode AFM image of the surface of a Ru(0001) thin film prior to graphene growth. (b) AFM image of the surface of a Ru(0001) thin film following graphene growth and electrochemical transfer. After the graphene transfer, the metal film has been annealed in vacuum at a typical graphene growth temperature (810 °C; 30 min). (c) Raman spectra of the samples shown in (a) and (b).

[1]K. S. Novoselov, A. K. Geim, S. V. Morozov, D. Jiang, Y. Zhang, S. V. Dubonos, I. V. Grigorieva, and A. A. Firsov, Science **306**, 666 (2004).

[2]A. K. Geim and K. S. Novoselov, Nature Mater. **6**, 183 (2007).

[3]R. R. Nair, P. Blake, A. N. Grigorenko, K. S. Novoselov, T. J. Booth, T. Stauber, N. M. R. Peres, and A. K. Geim, Science **320**, 1308 (2008).

[4]C. Lee, X. D. Wei, J. W. Kysar, and J. Hone, Science **321**, 385 (2008).

[5]J. C. Meyer, A. K. Geim, M. I. Katsnelson, K. S. Novoselov, T. J. Booth, and S. Roth, Nature **446**, 60 (2007).

[6]P. Avouris, Nano Lett. **10**, 4285 (2010).

[7]Y. Hernandez, V. Nicolosi, M. Lotya, F. M. Blighe, Z. Y. Sun, S. De, I. T. McGovern, B. Holland, M. Byrne, Y. K. Gun'ko, J. J. Boland, P. Niraj, G. Duesberg, S. Krishnamurthy, R. Goodhue, J. Hutchison, V. Scardaci, A. C. Ferrari, and J. N. Coleman, Nat. Nanotechnol. **3**, 563 (2008).

[8]K. V. Emtsev, A. Bostwick, K. Horn, J. Jobst, G. L. Kellogg, L. Ley, J. L. McChesney, T. Ohta, S. A. Reshanov, J. Rohrl, E. Rotenberg, A. K. Schmid, D. Waldmann, H. B. Weber, and T. Seyller, Nature Mater. **8**, 203 (2009).

[9]P. W. Sutter, J. I. Flege, and E. A. Sutter, Nature Mater. **7**, 406 (2008).

[10]P. Sutter, J. T. Sadowski, and E. Sutter, Phys. Rev. B **80**, 245411 (2009).

[11]L. B. Gao, W. C. Ren, H. L. Xu, L. Jin, Z. X. Wang, T. Ma, L. P. Ma, Z. Y. Zhang, Q. Fu, L. M. Peng, X. H. Bao, and H. M. Cheng, Nature Commun. **3**, 699 (2012).

[12]K. S. Kim, Y. Zhao, H. Jang, S. Y. Lee, J. M. Kim, K. S. Kim, J. H. Ahn, P. Kim, J. Y. Choi, and B. H. Hong, Nature **457**, 706 (2009).

[13]A. Reina, X. T. Jia, J. Ho, D. Nezich, H. B. Son, V. Bulovic, M. S. Dresselhaus, and J. Kong, Nano Lett. **9**, 30 (2009).

[14]X. Li, W. Cai, J. An, S. Kim, J. Nah, D. Yang, R. Piner, A. Velamakanni, I. Jung, E. Tutuc, S. K. Banerjee, L. Colombo, and R. S. Ruoff, Science **324**, 1312 (2009).

[15]S. Bae, H. Kim, Y. Lee, X. Xu, J.-S. Park, Y. Zheng, J. Balakrishnan, T. Lei, H. Ri Kim, Y. I. Song, Y.-J. Kim, K. S. Kim, B. Ozyilmaz, J.-H. Ahn, B. H. Hong, and S. Iijima, Nat. Nanotechnol. **5**, 574 (2010).

[16]Y. Wang, Y. Zheng, X. F. Xu, E. Dubuisson, Q. L. Bao, J. Lu, and K. P. Loh, ACS Nano **5**, 9927 (2011).

[17]P. Sutter and E. Sutter, Adv. Funct. Mater. **23**, 2617 (2013).

[18]E. Sutter, P. Albrecht, and P. Sutter, Appl. Phys. Lett. **95**, 133109 (2009).

[19]P. W. Sutter, P. M. Albrecht, and E. A. Sutter, Appl. Phys. Lett. **97**, 213101 (2010).

[20]P. Sutter, C. V. Ciobanu, and E. Sutter, Small **8**, 2250 (2012).

[21]P. Sutter, M. S. Hybertsen, J. T. Sadowski, and E. Sutter, Nano Lett. **9**, 2654 (2009).

[22]B. Wang, M.-L. Bocquet, S. Marchini, S. Günther, and J. Wintterlin, Phys. Chem. Chem. Phys. **10**, 3530 (2008).

[23]E. Sutter, P. Albrecht, B. Wang, M. L. Bocquet, L. J. Wu, Y. M. Zhu, and P. Sutter, Surf. Sci. **605**, 1676 (2011).

[24]P. Sutter, J. T. Sadowski, and E. A. Sutter, J. Am. Chem. Soc. **132**, 8175 (2010).

[25]P. Sutter, P. Albrecht, X. Tong, and E. Sutter, J. Phys. Chem. C **117**, 6320 (2013).

[26]X. Feng, S. Maier, and M. Salmeron, J. Am. Chem. Soc. **134**, 5662 (2012).

[27]B. Łosiewicz, M. Martin, C. Lebouin, and A. Lasia, J. Electroanal. Chem. **649**, 198 (2010).

[28]S. Hadži-Jordanov, H. Angerstein-Kozlowska, M. Vukovič, and B. E. Conway, J. Electrochem. Soc. **125**, 1471 (1978).

[29]A. M. El-Aziz and L. A. Kibler, Electrochem. Commun. **4**, 866 (2002).

[30]M. Ito and M. Nakamura, Faraday Discuss. **121**, 71 (2002).

[31]J. Mao, L. Huang, Y. Pan, M. Gao, J. He, H. Zhou, H. Guo, Y. Tian, Q. Zou, L. Zhang, H. Zhang, Y. Wang, S. Du, X. Zhou, A. H. C. Neto, and H.-J. Gao, Appl. Phys. Lett. **100**, 093101 (2012).

[32]A. C. Ferrari, J. C. Meyer, V. Scardaci, C. Casiraghi, M. Lazzeri, F. Mauri, S. Piscanec, D. Jiang, K. S. Novoselov, S. Roth, and A. K. Geim, Phys. Rev. Lett. **97**, 187401 (2006).

[33]X. Li, C. W. Magnuson, A. Venugopal, J. An, J. W. Suk, B. Han, M. Borysiak, W. Cai, A. Velamakanni, Y. Zhu, L. Fu, E. M. Vogel, E. Voelkl, L. Colombo, and R. S. Ruoff, Nano Lett. **10**, 4328 (2010).

[34]P. Y. Huang, C. S. Ruiz-Vargas, A. M. van der Zande, W. S. Whitney, M. P. Levendorf, J. W. Kevek, S. Garg, J. S. Alden, C. J. Hustedt, Y. Zhu, J. Park, P. L. McEuen, and D. A. Muller, Nature **469**, 389 (2011).

[35]X. Du, I. Skachko, A. Barker, and E. Y. Andrei, Nat. Nanotechnol. **3**, 491 (2008).

[36]C. R. Dean, A. F. Young, I. Meric, C. Lee, L. Wang, S. Sorgenfrei, K. Watanabe, T. Taniguchi, P. Kim, K. L. Shepard, and J. Hone, Nat. Nanotechnol. **5**, 722 (2010).